Applied Chemical Engineering (2025) Volume 8 Issue 2 ISSN: 2578-2010 (O)
doi: 10.59429/ace.v8i2.5663

RESEARCH ARTICLE

Ursolic acid alleviates alcohol induced nerve damage by regulating MAPK signaling pathway and extracellular matrix remodeling

Wei Zhu, Na Ge*

Department of Public Health, International College, Krirk University, Bangkok, Thailand

***Corresponding author:** Na Ge, Professor, genanihao80@163.com

ABSTRACT

The central nervous system (CNS) is one of the primary targets of alcohol-induced damage. Chronic alcohol consumption leads to cognitive deficits, motor impairments, anxiety-like behaviors, and even irreversible neuronal degeneration and death. However, therapeutic strategies for alcohol-related neurotoxicity remain limited, posing a significant public health concern. Ursolic acid (UA), with its antioxidant, anticancer, anti-inflammatory, hepatoprotective, and immunomodulatory properties, may confer protective effects against neurological damage. In this study, we established a zebrafish model of alcohol-induced neurotoxicity and investigated the potential of UA to mitigate neural injury. Using confocal live imaging in transgenic zebrafish lines, we observed that UA significantly alleviated alcohol-induced reductions in neuronal and dopaminergic neuron populations. Behavioral assays further demonstrated that UA restored normal locomotor activity in zebrafish embryos, indicating functional recovery of the nervous system. Transcriptomic sequencing revealed that UA ameliorated alcohol-induced neurotoxicity potentially by modulating the MAPK signaling pathway and promoting extracellular matrix (ECM) remodeling. This study provides experimental evidence for UA as a therapeutic candidate against alcohol-related neural damage and identifies potential molecular targets for clinical interventions.

Keywords: Ursolic acid; alcohol; nerve damage; zebrafish

ARTICLE INFO

Received: 8 May 2025
Accepted: 29 May 2025
Available online: 05 June 2025

1. Introduction

Approximately 2.3 billion people worldwide drink alcohol, and the central nervous system is one of the main target organs for alcohol damage. Drinking alcohol can lead to cognitive impairment, motor deficits, anxious behavior, and even irreversible damage such as neuronal degeneration and death[1]. In the central nervous system (CNS), alcohol damages the function of neurons and glial cells, causing many functional abnormalities such as neuronal death, cell migration, and glial cell differentiation, which may lead to dementia, cognitive impairment, motor impairment, anxious behavior, blood-brain barrier disorders, or nerve fiber demyelination[2,3]. The MRI imaging results of different drinking populations show that there is atrophy of the hippocampus, frontal cortex, pons, and cerebellum, as well as thinning of the corpus callosum. These structural abnormalities lead to various clinical symptoms such as psychological disorders, dementia, forgetfulness, and motor disorders in drinking populations[4][6], causing a heavy burden on society and families. Therefore, finding effective intervention measures to prevent and treat alcoholic nerve damage is one of the research hotspots.

Ursolic acid (UA) is a naturally occurring pentacyclic triterpenoid carboxylic acid compound widely found in plants such as hawthorn (Crataegus), sage (Salvia), privet (Ligustrum), papaya (Carica papaya). Current research has revealed that UA not only exhibits diverse biological activities, including antioxidant, anticancer, anti-inflammatory, hepatoprotective, and immunomodulatory effects[7-9], but also demonstrates high efficacy, safety, and low toxicity[10].

To date, studies on UA have primarily focused on its hepatoprotective and antitumor properties, with limited exploration in neurological and psychiatric disorders. In an MPTP-induced Parkinson's disease (PD) mouse model, MPTP administration led to behavioral abnormalities in pole-climbing and rotarod tests, accompanied by upregulated expression of microglial markers (Iba1), TNF-α, and the neuroinflammatory pathway NF-κB in the substantia nigra. UA treatment significantly ameliorated these behavioral deficits and suppressed neuroinflammatory responses[11]. Furthermore, UA promoted neuronal regeneration in mice following sciatic nerve transection, reducing muscle atrophy, increasing muscle fiber count and diameter, and accelerating neuromuscular junction reinnervation. Notably, both pre-treatment (10 days prior to injury) and immediate post-injury administration of UA effectively enhanced neuromuscular repair, with pre-treatment showing superior efficacy, highlighting UA's potential as both a preventive and therapeutic agent[12].

The zebrafish (Danio rerio) is a promising model organism in neurological damage research. Its utility in neuroscience has grown significantly because of its vertebrate status, with high physiological and genetic homology to humans, and similar central nervous system (CNS) morphology[13]. Most neuronal structures of mammals are conserved in the zebrafish, including somatic cells, dendrites, myelinated or unmyelinated axons, and the blood-brain barrier[14,15]. The physiological characteristics and permeability of the blood-brain barrier are also similar to those of mammals. Neurotransmitters are highly conserved compared to humans[15,16]. Zebrafish embryos developed in vitro are transparent, making it easy to observe the distribution and activity of various cells in real-time through in vivo imaging. Combined with fluorescent protein labeling technology, we can observe phenomena such as nerve growth and synaptic development.

Although UA exhibits neuroprotective effects, its role in alleviating alcohol-induced neural damage remains underexplored. Therefore, this study establishes a zebrafish alcohol-induced neurotoxicity model to investigate whether UA mitigates alcohol-related neural damage and elucidate its underlying mechanisms.

2. Materials and methods

2.1. Zebrafish feeding and maintenance

Wild-type (WT) zebrafish strains Tubingen[17] and WIK, the transgenic zebrafish line *Tg(HuC: eGFP)* and *Tg(Vmat2: eGFP)* were described previously. The *Tg(Vmat2: eGFP)* transgenic fish line was a kind gift from professor Jiulin Du (Center for Excellence in Brain Science and Intelligence Technology, Chinese Academy of Sciences). The zebrafish were maintained in a circulating water filtration system at a pH of 7.0 ± 1.0, water temperature of 28 ± 1 °C, and a 12-h light/dark cycle. The zebrafish were fed shrimp twice daily. The night before the experiment, the male and female fish were placed in the same incubator and separated by a comb. At 8:30 am on the following day, the zebrafish began to spawn. To prevent melanin pigment formation, embryos were incubated in egg water containing 0.045% 1-phenyl-2-thiourea (PTU, Sigma) after 1 dpf (day post-fertilization, dpf) and change the egg water every day. The embryos were collected at the desired stages[18]. The zebrafish used in this study were maintained in the model animal platform at the Centre of Translational Medicine in Baotou Medical College. This study was reviewed and approved by the Experimental Animal Ethics Committee of the Baotou Medical College, Inner Mongolia University of Science and Technology, Inner Mongolia, China.

2.2. Drug preparation

Ursolic acid (UA) (purity ≥ 98 %, CAS No: 77-52-1) was purchased from the Xi'an Realin Biotechnology Co., Ltd., China. Dissolved 0.21g of UA in 30ml DMSO and sonicated. The storage concentration is 6.86 mg/ml. The concentrations used in each experiment are individually labeled.

2.3. Establishment of zebrafish alcohol injury model and ursolic acid treatment

After approximately 3 dpf, collected embryos were randomly divided into 6 well plates containing 30 embryos per well. The embryos were then subjected to 1.5% (v/v) ethanol and co-exposed with ursolic acid for 2 days. We have selected the dose based on ursolic acid toxicity on zebrafish embryos. After 2 days of co-exposure, the embryos were transferred to new 6-well plates and washed thoroughly to remove the traces of ethanol and ursolic acid. Then zebrafish embryos were collected for observation and other experiments.

2.4. Zebrafish embryos toxicity assay

Starting with the different concentration ursolic acid, directly observed each-well every 24 hours under a stereo microscope (Nikon, SMZ18) connected to a camera device at specific time points (24, 48, 72, 96 and 120 hpf). After 120 hpf, larvae were anesthetized in 0.02 % tricaine and embedded in 1% low-melt agarose gel, then the larvae were positioned on the lateral side and photographed to assess morphology.

2.5. Real-time observation of neuron and dopaminergic neuron in zebrafish embryo

The neuron and dopaminergic neuron image were observed after 1.5% ethanol and 12.5 μg/mL UA treatment using Tg(*HuC:eGFP*) and Tg(*Vmat2:eGFP*). The zebrafish embryos were anaesthetised with tricaine (0.08% by volume), mounted in a low-melting agarose gel (0.5%), and live imaging of the neuron and dopaminergic neuron were performed using a confocal microscope (A1+ confocal microscope, Nikon, Japan).

2.6. Analysis of zebrafish behaviour

Embryos were placed in a 24-well plate containing zebrafish culture solution (1 mL/well). Zebrafish embryo movement was recorded for 15 min using a behavioural instrument (Noldus, Holland). EthoVision® XT software was used to determine the motion-speed parameters. The experiment was repeated at least thrice.

2.7. Transcriptome sequencing

Transcriptome sequencing of zebrafish embryos in the three groups was performed by Shanghai Applied Protein Technology (Shanghai, China), and changes in the differentially expressed genes (DEGs) were analysed. Wild type zebrafish embryos (N=30) were collected at 5 dpf after treated with ethanol and UA, respectively. Total RNA was extracted from the tissue using TRIzol® Reagent according the manufacturer's instructions (Magen) and genomic DNA was removed using DNase I (TaKara). Then RNA quality was determined by Agilent Bioanalyzer 4150 system (Agilent Technologies, CA, USA) and quantified using the Nanodrop ND-2000 system (Thermo Scientific, USA). Only high-quality RNA sample (OD260/280 = 1.8~2.2, OD260/230 ≥ 2.0, RIN ≥ 6.5, 28 S:18S ≥ 1.0, >1 μg) was used to construct sequencing library. RNA-seq transcriptome library was prepared following ABclonal mRNA-seq Lib Prep Kit (ABclonal, China) using 1 μg of total RNA. PCR products were purified (AMPure XP system) and library quality was assessed on an Agilent Bioanalyzer 4150 system. Finally, the library preparations were sequenced on an Illumina NovaSeq 6000 and 150 bp paired-end reads were generated. The data generated from Illumina platform were used for bioinformatics analysis.

2.8. Statistical analysis

Statistical analysis was performed by Graphpad Prism 8 software using the two-tailed Student's *t*-test and *P* value of less than 0.05 was considered significant. Error values were calculated by standard error of the mean (SEM).

3. Results

3.1. Successful construction of the ethanol injury model

To investigate the neurological damage caused by alcohol, we first established an alcohol-induced injury model in zebrafish. Zebrafish embryos were treated with ethanol at varying concentrations (1%, 1.5%, 2%, 2.5%, 3% and 4%), and their mortality and malformation rates were recorded. As shown in **Figure 1A-1B**, the mortality rate of embryos shows a dose-dependent pattern. The mortality increased progressively with higher ethanol concentrations: 1.5% ethanol resulted in a mortality rate of 2.67%, while 2.5% ethanol caused 65.33% mortality. The calculated median lethal concentration (LC50) for ethanol was 2.37%. Morphological analysis revealed that embryos exposed to 2% ethanol exhibited severe pericardial edema, shortened body length, and axial curvature, whereas those treated with ≤1.5% ethanol showed no significant morphological abnormalities (**Figure 1C**).

Behavioral assays further demonstrated impaired locomotor activity in embryos exposed to ≥2% ethanol, characterized by reduced movement trajectories. In contrast, embryos treated with ≤1.5% ethanol retained nearly normal motor function (**Figure 1D**). Based on these findings, 1.5% ethanol was selected for subsequent neurotoxicity experiments.

Figure 1

A

EtOH (%)	Mortality rate (%)
0	0
1.0	1.33
1.5	2.67
2.0	13.33
2.5	65.33
3.0	100.00
4.0	100.00

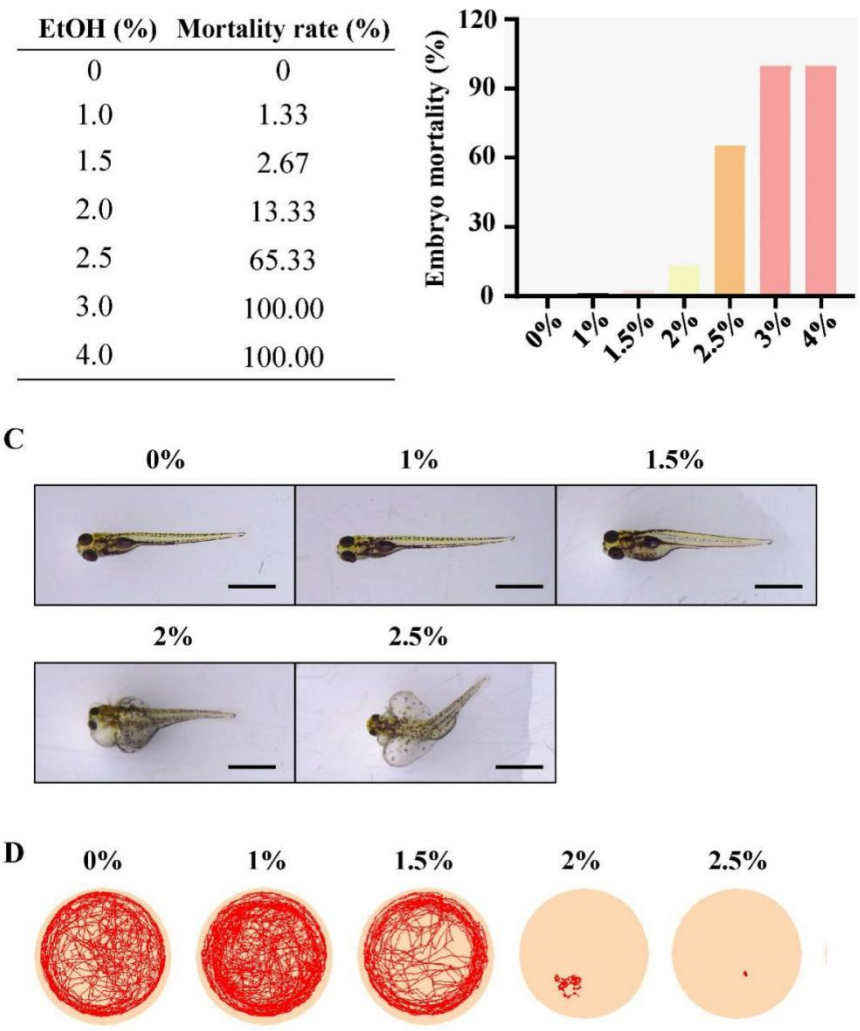

Figure 1. Establishment of the alcohol-induced injury model.

Ethanol toxicity assays to determine survival rate in zebrafish embryos exposed to alcohol (A, B). Morphological malformations in zebrafish under varying alcohol concentrations (C). Behavioral trajectory maps of zebrafish under different alcohol concentrations (D).

3.2. Selection of therapeutic concentration of UA

To determine the appropriate dosage of ursolic acid (UA) for zebrafish, a toxicity assessment was conducted. Embryos were treated with UA at concentrations ranging from 10 to 50 μg/mL. As shown in **Figures 2A-2B**, malformation and mortality rates escalated with increasing UA doses. At 40 μg/mL UA, mortality reached 85.7%, and the calculated LC50 was 34.44 μg/mL. Time-course mortality analysis indicated no death or malformation in embryos treated with ≤20 μg/mL UA over 5 days (**Figure 2C**). Morphological observations (**Figure 2D**) revealed pericardial edema at 20 μg/mL ursolic acid. And body curvature could be found at 30 μg/mL UA, which worsened at 40 μg/mL, while embryos exposed to ≤20 μg/mL appeared normal. Consequently, 12.5 μg/mL UA was chosen for further experiments.

Figure 2

A

UA (μg/ml)	Mortality rate (%)
0.00	0
10	0
12.5	0
20	0
30	18.7
40	85.7
50	100.00

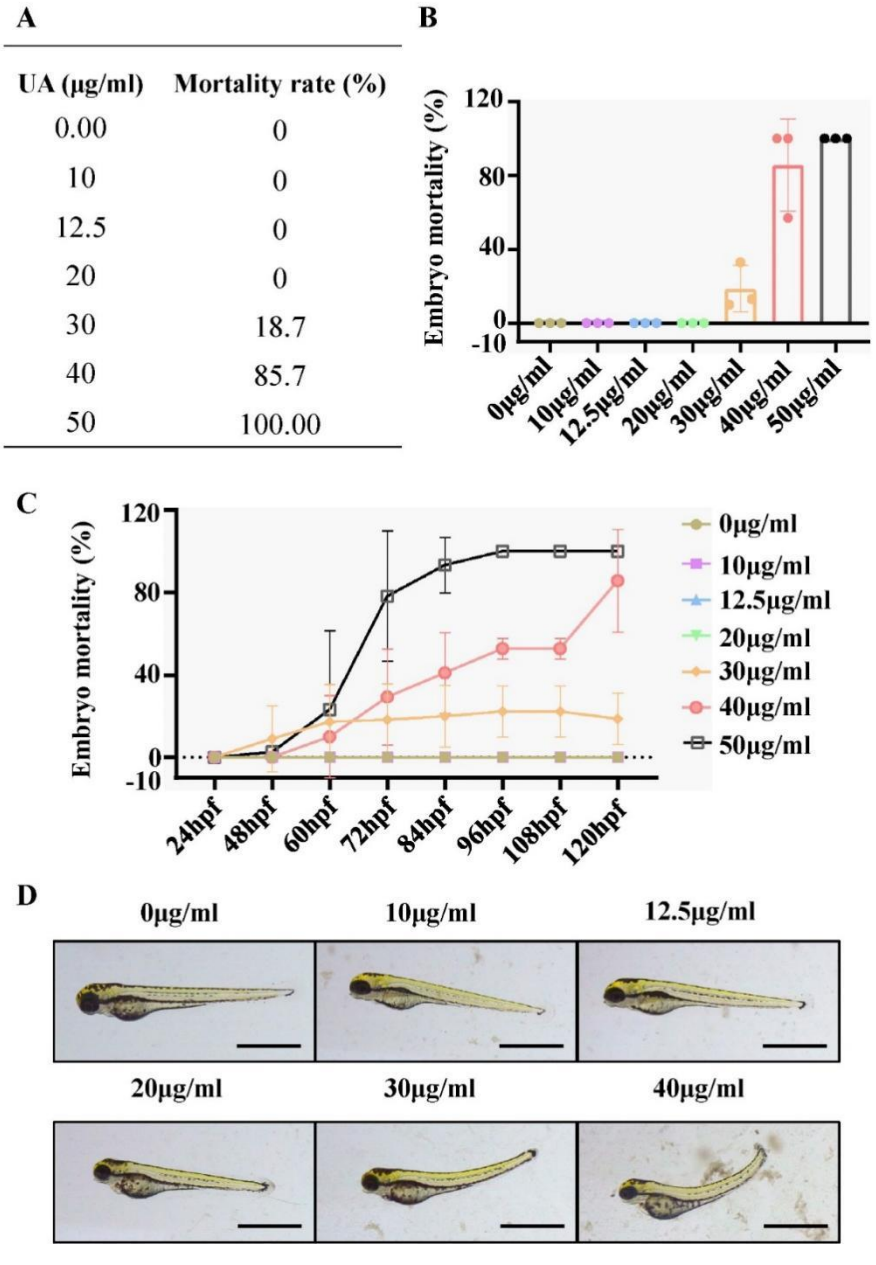

Figure 2. Toxicological evaluation of ursolic acid (UA) intervention concentrations.

UA toxicity assays to identify survival rate and optimal therapeutic concentrations in zebrafish embryos (A, B). Survival rates observed across different treatment durations (C). Morphological malformations in zebrafish under varying alcohol concentrations with UA intervention (D). *, $P < 0.05$; **, $P < 0.01$; ***, $P < 0.001$.

3.3. UA can alleviate nerve damage caused by alcohol

Based on the experiments, the following protocol was established: zebrafish at 3 days post-fertilization (dpf) were treated with 1.5% ethanol to induce a neural injury model, while simultaneously administered 12.5 μg/mL ursolic acid (UA) as a therapeutic intervention (**Figure 3A**). As shown in **Figure 3B**, UA effectively alleviated ethanol-induced pericardial edema. To assess neurological damage, the transgenic zebrafish line Tg(*HuC:*eGFP), which labels all neurons with green fluorescent protein (GFP), was utilized. Ethanol exposure significantly reduced GFP-labeled neuronal density, whereas UA treatment protected neuronal populations (**Figure 3C**), with statistical data presented in **Figure 3E**.

Additionally, the dopaminergic neuron-specific transgenic line Tg(*Vmat2:eGFP*) was employed to evaluate changes in dopaminergic neurons. Ethanol treatment similarly caused a marked reduction in dopaminergic neurons, which was prevented by UA administration (**Figure 3D**). Quantitative results are detailed in **Figure 3F**.

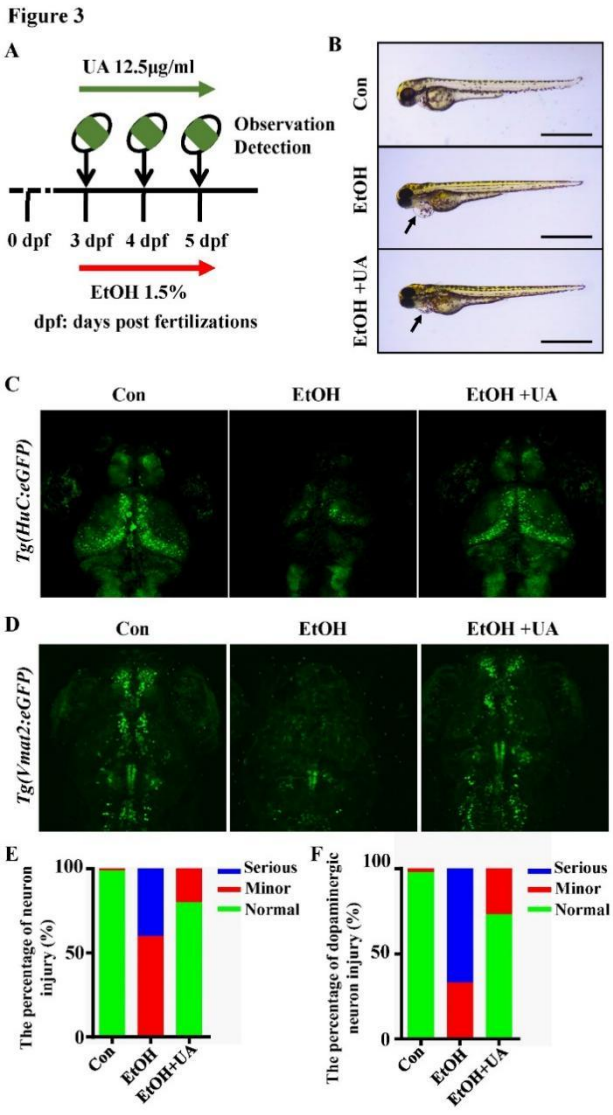

Figure 3. UA alleviates alcohol-induced neuronal damage.

Schematic diagram of the experimental design (A). Morphological changes in zebrafish embryos following alcohol exposure and UA intervention (B). Confocal microscopy images showing neuronal changes in the transgenic line Tg(*HuC:eGFP*) (C). Confocal microscopy images of dopaminergic neurons in the transgenic line Tg(*Vmat2:eGFP*) (D). E Quantitative analysis of total neurons. F Quantitative analysis of dopaminergic neurons.

3.4. UA effectively protected neuron function

To determine whether UA-mediated prevent of ethanol-induced neural damage correlated with functional restoration, locomotor activity was analyzed. **Figure 4A** demonstrates that ethanol-exposed embryos exhibited significantly impaired swimming behavior, including reduced travel distance and velocity. We conducted a detailed classification and description of behavioral data, dividing the locomotion damage caused by alcohol into three levels. And we performed statistical analysis on the protective proportion for each level, as shown in **Figures 4B**. In contrast, UA-treated embryos showed restored locomotor performance, with both path length and swimming speed returning to near-normal levels (**Figure 4C-4D**). Alcohol causes a significant decrease in maximum acceleration and maximum rotation angle, while UA can partially recover the loss of maximum acceleration and maximum rotation angle **(Figure 4E-4F**).

Figure 4

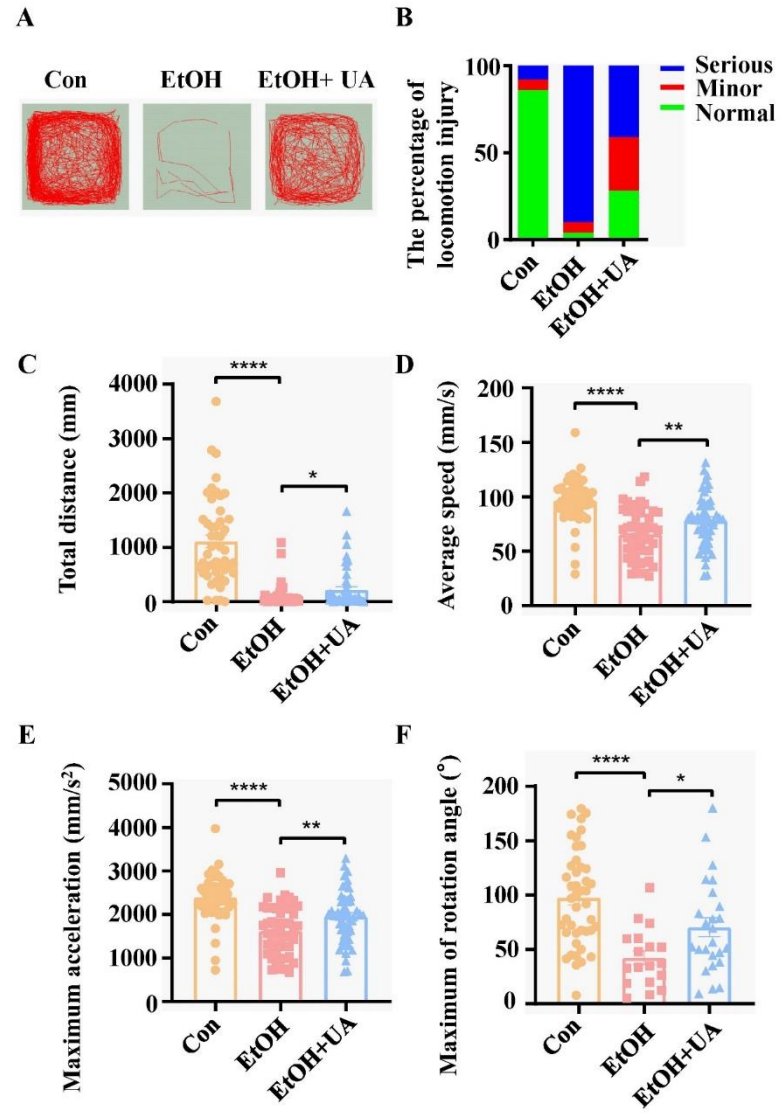

Figure 4. UA ameliorates alcohol-induced locomotor deficits.

Locomotor trajectory maps of zebrafish embryos (A). Proportion of alcohol damaged embryos, respectively (B). Statistical analysis of total movement distance (C). Statistical analysis of average speed (D). Statistical analysis of maximum acceleration (E). Statistical analysis of maximum of rotation angle (F). *, $P < 0.05$; **, $P < 0.01$; ****, $P < 0.0001$.

3.5. Transcriptome sequencing

To explore mechanisms and identify the specific genes or molecular pathways through which ursolic acid (UA) exerts its therapeutic effects, we performed transcriptomic sequencing. First, we assessed the quality of sequencing samples using Principal Component Analysis (PCA) to evaluate inter-group differences and intra-group reproducibility/homogeneity. As shown in **Figure 5A**, samples from the three groups (control, ethanol model, and UA-treated) clustered distinctly between groups but tightly within groups, indicating robust inter-group variability and intra-group consistency.

A hierarchical clustering heatmap (**Figure 5B**) visualized gene expression trends across samples. Deeper red hues denoted stronger upregulation, while deeper blue hues indicated downregulation. The heatmap confirmed uniform expression patterns within control, EtOH, and UA-treated groups. Both PCA and heatmap analyses validated the stability and reliability of transcriptomic data, supporting further differential gene analysis.

We screened for differentially expressed genes (DEGs) based on the following criteria: $P < 0.05$, Log_2FC fold change >1 or <-1. To identify shared differentially expressed genes (DEGs) across groups, a Venn diagram was constructed. We found 51 overlapping DEGs between the EtOH vs. Control and UA vs. EtOH comparisons (**Figure 5C**). Volcano plots (**Figure 5D**) revealed that EtOH exposure induced significant changes in 1074 transcripts compared to controls (820 upregulated, 254 downregulated). UA treatment reversed 268 transcripts in the EtOH group (145 upregulated, 123 downregulated). Among these 51 overlapping DEGs, 42 genes exhibited different changing trends in different groups, either upregulate first and then downregulate, or downregulate first and then upregulate. Among the 42 genes with inconsistent trends, some genes were not annotated, and 20 of them caught our attention. Notably, comparing simultaneous use of EtOH/UA with EtOH, 20 DEGs showed opposing expression trends to comparing EtOH with control, which means the usage of UA reverses EtOH-induced gene expression changes.

Figure 5

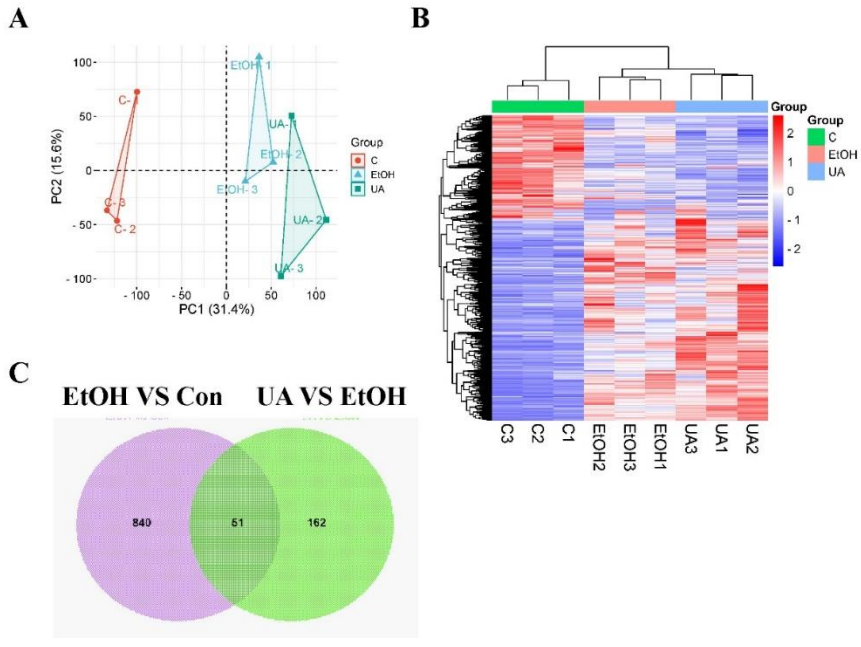

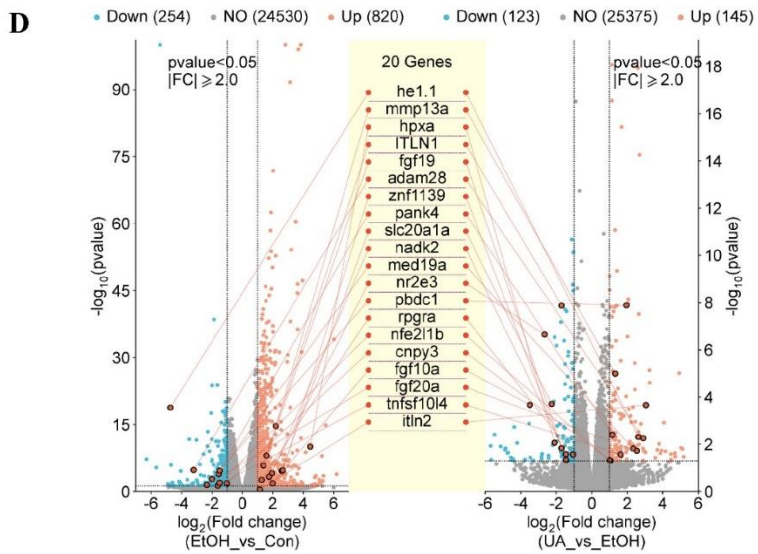

Figure 5. Transcriptome sequencing.

(A) Principal component analysis (PCA) of nine samples from three groups. (B) Heat map showing all the differentially expressed genes (DEGs) identified by RNA-sequencing. (C) Venn plot showing the strategy for screening the opposite DEGs in EtOH and UA group. (D)Volcano plot showing the differentially expressed genes (DEGs) (criteria: $P < 0.05$, $\log_2$ fold change >1 or <-1) altered in EtOH group and the UA treatment group.

Gene Ontology (GO) analysis of the 51 overlapping DEGs (**Figure 6A**) highlighted enrichment. In Biological Processes (BP), the most enriched genes directions include: Positive regulation of gene expression, cholesterol biosynthesis, sterol biosynthesis. In Cellular Components (CC), the most enriched genes directions include: Extracellular matrix, apical plasma membrane, lipid droplets, collagen-containing extracellular matrix. In Molecular Functions (MF), the most enriched genes directions include: L-threonyl-aminoacyl-tRNA synthetase activity, growth factor activity, organic acid binding.

A bubble plot (**Figure 6B**) further emphasized pathways linked to extracellular matrix remodeling, gene expression regulation, cholesterol/sterol biosynthesis, fibroblast growth factor receptor (FGFR) signaling, and protein phosphorylation. The fibroblast growth factor receptor (FGFR) signaling and extracellular matrix remodeling are relevant to neural repair and spinal cord injury recovery.

KEGG pathway analysis (**Figure 6C**) identified key pathways associated with alcohol-induced injury and UA-mediated recovery, including steroid metabolism, MAPK signaling, cytoskeleton synthesis, calcium signaling, and terpenoid backbone biosynthesis.

Figure 6

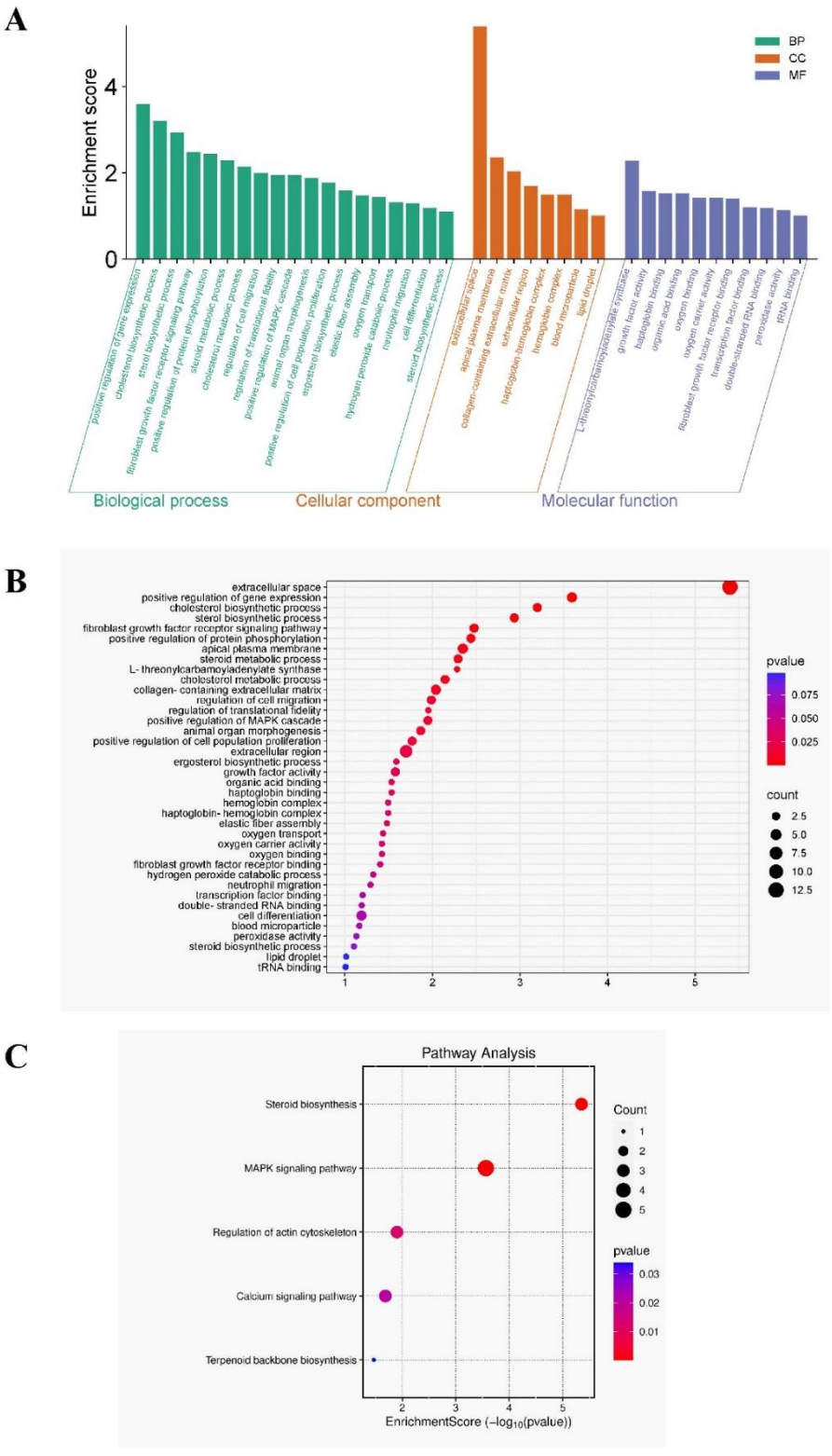

Figure 6. Bioinformatics analyses.

Gene ontology (GO) and Kyoto Encyclopedia of Genes and Genomes (KEGG) analyses show the enrichment results of the 46 opposite DEGs obtained in **Figure 5**. (A and B) Gene ontology (GO) analyses. (C) Kyoto Encyclopedia of Genes and Genomes (KEGG) analyses.

4. Discussion

In this study, we established a zebrafish ethanol-induced neural injury model and demonstrated that ursolic acid (UA) alleviates alcohol-associated neural damage and protects locomotor function. Transcriptomic analysis revealed that UA neuroprotective effects are likely mediated by the regulation of the MAPK signaling pathway and extracellular matrix (ECM) remodeling.

Zebrafish are sensitive to alcohol, respond to reward stimuli, and tolerate and exhibit withdrawal behaviors. Thus zebrafish have emerged as a prominent model organism for studying alcohol-induced damage, due to their high conservation with humans in alcohol absorption, metabolism, and sensitivity. Recent studies have shown that the Non-Steroidal Anti-Inflammatory Drug (NSAID) benzydamine alleviates ethanol-induced teratogenesis in early zebrafish embryos, suggesting its therapeutic potential for fetal alcohol spectrum disorders (FASD) caused by prenatal alcohol exposure[19]. The pharmacological modulation of opioids on behavioral and neurobiological aspects was evaluated when repeated exposure to ethanol and treated with naltrexone in adult zebrafish[20]. These results in zebrafish provide a better understanding of the neurophysiological and behavioral changes caused by repetitive alcohol use.

In a mouse spinal cord injury model, UA enhances motor recovery and axonal regeneration by activating the MAPK/PI3K/mTOR signaling pathway, reducing levels of proinflammatory markers (IL-6 and TNF-α), and suppressing astrocyte proliferation[21]. In rat middle cerebral artery occlusion/reperfusion (MCAO/R) models and oxygen-glucose deprivation/reoxygenation (OGD-R)-treated SH-SY5Y cell models, UA acts as a peroxisome proliferator-activated receptor gamma (PPARγ) agonist. It alleviates cerebral ischemia-reperfusion injury by suppressing the activation of the p38/pERK/pJNK/MAPK signaling pathway and restoring the balance between matrix metalloproteinases (MMPs) and tissue inhibitor of metalloproteinase 1 (TIMP1)[22,23]

The protective effect of ursolic acid on the nervous system may also be mediated through other signaling pathways. In rat intracerebral hemorrhage (ICH) models and BV2 microglial cell experiments, UA inhibits M1 microglial polarization and decreases levels of p-NF-κB, GSDMD-N, cleaved caspase-1, TNF-α, IL-6, and IL-1β. UA attenuates post-ICH neuroinflammation by suppressing microglial pyroptosis via the NF-κB/NLRP3/GSDMD pathway[24].

Another rat ischemia-reperfusion study demonstrated that UA reduces proinflammatory cytokine production (IL-1β, TNF-α, and IL-6) via the HMGB1/TLR4/NF-κB pathway, thereby protecting against cerebral ischemia-reperfusion injury[25]. These findings collectively highlight UA's neuroprotective roles through multi-pathway regulation.

The protective mechanism of ursolic acid against alcohol induced nerve damage still needs further research. This study provides preliminary experimental data for the promotion and application of using ursolic acid to develop new drugs and functional foods for further research on the protection of alcoholic nerve damage.

Author Contribution

WZ and NG designed research, analyzed data; WZ performed experiments and wrote the manuscript.

Acknowledgements

We thank Jiulin Du professor (Center for Excellence in Brain Science and Intelligence Technology, Chinese Academy of Sciences) for the gifting the transgenic fish line Tg(*Vmat2: eGFP*).

Funding

This work was supported by Inner Mongolia High School Science Research Foundation (NJZY23093), Research and Development Funds of Baotou Medical College (BYJJ-ZRQM202419, BYJJ-GCJH202501), and college student project (HLJH202506).

Competing Interests

The author reports no conflicts of interest in this work.

Additional Information

Correspondence and requests for materials should be addressed to Na Ge.

Declarations

Ethics approval and consent to participate.

This study was reviewed and approved by the Experimental Animal Ethics Committee of the Baotou Medical College, Inner Mongolia University of Science and Technology, Inner Mongolia, China.

Consent for publication

Not applicable.

Availability of data and materials

The data used to support the findings of this study are included within the article.

Figure legend

Figure 1. Establishment of the alcohol-induced injury model.

Ethanol toxicity assays to determine survival rate in zebrafish embryos exposed to alcohol (A, B). Morphological malformations in zebrafish under varying alcohol concentrations (C). Behavioral trajectory maps of zebrafish under different alcohol concentrations (D).

Figure 2. Toxicological evaluation of ursolic acid (UA) intervention concentrations.

UA toxicity assays to identify survival rate and optimal therapeutic concentrations in zebrafish embryos (A, B). Survival rates observed across different treatment durations (C). Morphological malformations in zebrafish under varying alcohol concentrations with UA intervention (D). *, $P < 0.05$; **, $P < 0.01$; ***, $P < 0.001$.

Figure 3. UA alleviates alcohol-induced neuronal damage.

Schematic diagram of the experimental design (A). Morphological changes in zebrafish embryos following alcohol exposure and UA intervention (B). Confocal microscopy images showing neuronal changes in the transgenic line Tg(*HuC:eGFP*) (C). Confocal microscopy images of dopaminergic neurons in the transgenic line Tg(*Vmat2:eGFP*) (D). E Quantitative analysis of total neurons. F Quantitative analysis of dopaminergic neurons.

Figure 4. UA ameliorates alcohol-induced locomotor deficits.

Locomotor trajectory maps of zebrafish embryos (A). Proportion of alcohol damaged embryos, respectively (B). Statistical analysis of total movement distance (C). Statistical analysis of average speed (D). Statistical analysis of maximum acceleration (E). Statistical analysis of maximum of rotation angle (F). *, $P < 0.05$; **, $P < 0.01$; ****, $P < 0.0001$.

Figure 5. Transcriptome sequencing.

(A) Principal component analysis (PCA) of nine samples from three groups. (B) Heat map showing all the differentially expressed genes (DEGs) identified by RNA-sequencing. (C) Venn plot showing the strategy for screening the opposite DEGs in EtOH and UA group. (D)Volcano plot showing the differentially expressed genes (DEGs) (criteria: $P < 0.05$, $\log_2$ fold change >1 or <-1) altered in EtOH group and the UA treatment group.

Figure 6. Bioinformatics analyses.

Gene ontology (GO) and Kyoto Encyclopedia of Genes and Genomes (KEGG) analyses show the enrichment results of the 46 opposite DEGs obtained in **Figure 5**. (A and B) Gene ontology (GO) analyses. (C) Kyoto Encyclopedia of Genes and Genomes (KEGG) analyses.

References

1. Rodriguez-Gonzalez, A. & Orio, L. Microbiota and Alcohol Use Disorder: Are Psychobiotics a Novel Therapeutic Strategy? Current pharmaceutical design 26, 2426-2437, doi:10.2174/1381612826666200122153541 (2020).
2. Cohen, A. C., Tong, M., Wands, J. R. & de la Monte, S. M. Insulin and insulin-like growth factor resistance with neurodegeneration in an adult chronic ethanol exposure model. Alcoholism, clinical and experimental research 31, 1558-1573, doi:10.1111/j.1530-0277.2007.00450.x (2007).
3. Tiwari, V. & Chopra, K. Resveratrol abrogates alcohol-induced cognitive deficits by attenuating oxidative-nitrosative stress and inflammatory cascade in the adult rat brain. Neurochemistry international 62, 861-869, doi:10.1016/j.neuint.2013.02.012 (2013).
4. Buhler, M. & Mann, K. Alcohol and the human brain: a systematic review of different neuroimaging methods. Alcoholism, clinical and experimental research 35, 1771-1793, doi:10.1111/j.1530-0277.2011.01540.x (2011).
5. Zuccoli, G. et al. Neuroimaging findings in alcohol-related encephalopathies. AJR. American journal of roentgenology 195, 1378-1384, doi:10.2214/AJR.09.4130 (2010).
6. Zahr, N. M. & Pfefferbaum, A. Alcohol's Effects on the Brain: Neuroimaging Results in Humans and Animal Models. Alcohol research : current reviews 38, 183-206 (2017).
7. Iqbal, J. et al. Ursolic acid a promising candidate in the therapeutics of breast cancer: Current status and future implications. Biomedicine & pharmacotherapy = Biomedecine & pharmacotherapie 108, 752-756, doi:10.1016/j.biopha.2018.09.096 (2018).
8. Ku, C. M. & Lin, J. Y. Anti-inflammatory effects of 27 selected terpenoid compounds tested through modulating Th1/Th2 cytokine secretion profiles using murine primary splenocytes. Food chemistry 141, 1104-1113, doi:10.1016/j.foodchem.2013.04.044 (2013).
9. Tan, J., Huang, W., Chen, S. L. & Yue, Y. [Synthesis and anti-inflammatory activity of ursolic acid derivative-chalcone conjugates]. Yao xue xue bao = Acta pharmaceutica Sinica 51, 938-946 (2016).
10. Cargnin, S. T. & Gnoatto, S. B. Ursolic acid from apple pomace and traditional plants: A valuable triterpenoid with functional properties. Food chemistry 220, 477-489, doi:10.1016/j.foodchem.2016.10.029 (2017).
11. Rai, S. N. et al. Anti-inflammatory Activity of Ursolic Acid in MPTP-Induced Parkinsonian Mouse Model. Neurotoxicity research 36, 452-462, doi:10.1007/s12640-019-00038-6 (2019).
12. Iannuzzo, F. et al. Therapeutic Effect of an Ursolic Acid-Based Nutraceutical on Neuronal Regeneration after Sciatic Nerve Injury. International journal of molecular sciences 25, doi:10.3390/ijms25020902 (2024).
13. Kalueff, A. V., Stewart, A. M. & Gerlai, R. Zebrafish as an emerging model for studying complex brain disorders. Trends in pharmacological sciences 35, 63-75, doi:10.1016/j.tips.2013.12.002 (2014).
14. Cuoghi, B. & Mola, L. Microglia of teleosts: facing a challenge in neurobiology. European journal of histochemistry : EJH 51, 231-240 (2007).
15. Wager, K. & Russell, C. Mitophagy and neurodegeneration: the zebrafish model system. Autophagy 9, 1693-1709, doi:10.4161/auto.25082 (2013).
16. Bretaud, S., MacRaild, S., Ingham, P. W. & Bandmann, O. The influence of the zebrafish genetic background on Parkinson's disease-related aspects. Zebrafish 8, 103-108, doi:10.1089/zeb.2011.0697 (2011).
17. Vinciguerra, P., Iglesias, N., Camblong, J., Zenklusen, D. & Stutz, F. Perinuclear Mlp proteins downregulate gene expression in response to a defect in mRNA export. The EMBO journal 24, 813-823, doi:10.1038/sj.emboj.7600527 (2005).
18. Kimmel, C. B., Ballard, W. W., Kimmel, S. R., Ullmann, B. & Schilling, T. F. Stages of embryonic development of the zebrafish. Developmental dynamics : an official publication of the American Association of Anatomists 203, 253-310, doi:10.1002/aja.1002030302 (1995).
19. Dasgupta, T., Manickam, V. & Tamizhselvi, R. Benzydamine rescues ethanol-induced teratogenesis in zebrafish FASD model. Scientific reports 15, 9066, doi:10.1038/s41598-025-93539-8 (2025).

20. Bernardo, H. T. et al. Naltrexone Alters Neurochemical and Behavioral Parameters in a Zebrafish Model of Repeated Alcohol Exposure. Neurochemical research 50, 97, doi:10.1007/s11064-025-04349-3 (2025).
21. Sahu, S., Li, R., Kadeyala, P. K., Liu, S. & Schachner, M. The human natural killer-1 (HNK-1) glycan mimetic ursolic acid promotes functional recovery after spinal cord injury in mouse. The Journal of nutritional biochemistry 55, 219-228, doi:10.1016/j.jnutbio.2018.01.016 (2018).
22. Qiu, L. et al. Ursolic Acid Ameliorated Neuronal Damage by Restoring Microglia-Activated MMP/TIMP Imbalance in vitro. Drug design, development and therapy 17, 2481-2493, doi:10.2147/DDDT.S411408 (2023).
23. Wang, Y., He, Z. & Deng, S. Ursolic acid reduces the metalloprotease/anti-metalloprotease imbalance in cerebral ischemia and reperfusion injury. Drug design, development and therapy 10, 1663-1674, doi:10.2147/DDDT.S103829 (2016).
24. Lei, P. et al. Ursolic Acid Alleviates Neuroinflammation after Intracerebral Hemorrhage by Mediating Microglial Pyroptosis via the NF-kappaB/NLRP3/GSDMD Pathway. International journal of molecular sciences 24, doi:10.3390/ijms241914771 (2023).
25. Wang, Y., Li, L., Deng, S., Liu, F. & He, Z. Ursolic Acid Ameliorates Inflammation in Cerebral Ischemia and Reperfusion Injury Possibly via High Mobility Group Box 1/Toll-Like Receptor 4/NFkappaB Pathway. Frontiers in neurology 9, 253, doi:10.3389/fneur.2018.00253 (2018).